

Adsorbate core-level azimuthal photoelectron diffraction at intermediate energies of 230–900 eV: Grazing emission with polarization dependence

B. Sinković, P. J. Orders,* C. S. Fadley, and R. Trehan

Department of Chemistry, University of Hawaii, Honolulu, Hawaii 96822

Z. Hussain

Department of Physics, University of Petroleum and Minerals, Dhahran, Saudi Arabia

J. Lecante

Service de Physique des Atomes et des Surfaces, Centre d'Etudes Nucléaires de Saclay, F-91191 Gif-sur-Yvette, France and Laboratoire pour l'Utilisation du Rayonnement Electromagnétique, Centre National de la Recherche Scientifique, F-91405 Orsay, France

(Received 25 July 1983)

Synchrotron radiation in the energy range 2700–3400 eV is used to study adsorbate core-level azimuthal x-ray photoelectron diffraction (XPD) in the as-yet-unexplored kinetic-energy range from 230 to 900 eV. The well-defined $c(2 \times 2)S$ overlayer on Ni(001) is studied at 10° grazing electron emission and with two radiation orientations: s polarization and a specially selected p polarization maximally emphasizing substrate Ni scattering relative to the primary wave. Pronounced XPD effects of 27–47% are observed in both cases. The s -polarization results are well described by a simple single-scattering model over the full energy range, although sensitivity to adsorbate vertical position is predicted to be low unless the adsorbate is within $\lesssim 1.0 \text{ \AA}$ of the Ni surface. Corresponding p -polarization results at 230 eV are markedly different in features and exhibit higher anisotropies. In order to be semiquantitatively described by theory, the p -polarization data require a reduction in scattering amplitudes, possibly due to inelastic effects, and the inclusion of double-scattering events. In p polarization, a higher sensitivity to adsorbate vertical positions is found. Both sets of data are consistent with the known structure of this overlayer.

Prior studies of azimuthal photoelectron diffraction from adsorbate core levels have been limited to two separate kinetic-energy regimes: $\geq 1000 \text{ eV}$ using standard unpolarized x-ray sources^{1–3} and $\leq 100 \text{ eV}$ using synchrotron radiation.^{4,5} Although both groups of studies have suggested that useful information concerning surface atomic geometries can be derived, the previous x-ray photoelectron diffraction (XPD) work has demonstrated certain attractive features of carrying out such measurements at higher energies.^{1,3} In particular, a simple single-scattering or kinematical model provides a very good description of the diffraction features observed at electron kinetic energies of $\sim 10^3 \text{ eV}$. At such high energies, forward scattering dominates, and this can produce rather directly interpretable peaks due to nearest-neighbor scatterers.^{2,3} However, because forward scattering is required, grazing emission angles with respect to the surface must be used. By contrast, in the lower-energy regime using uv excitation, rather complex multiple scattering theory has been necessary for interpreting data^{4,5} and one also expects large-angle or backscattering events to be much more important. Thus, larger take-off angles with respect to the surface may be utilized.

In the present study, we have performed the first intermediate-energy azimuthal XPD measurements using variable-polarization synchrotron radiation for excitation. The very well-characterized system of $c(2 \times 2)S$ on Ni(001) was used as a test case, since the bonding

geometry of S has previously been determined to be in fourfold hollow sites at 1.30–1.37 Å above the Ni surface plane.⁶ The previously unexplored kinetic-energy range from 230–900 eV was investigated in grazing emission geometries with a 10° polar angle of electron emission with respect to the surface. Two extreme polarization orientations also were studied to determine their effects on the observed XPD patterns and the degree of structural sensitivity achieved. The validity of a kinematical model for describing such data has also been tested by detailed comparisons to the results of single-scattering cluster (SSC) calculations and, in one case, also calculations including double-scattering (DS) events.

The experiments were performed on the 2° beam line of the Stanford Synchrotron Radiation Laboratory using the Ge(111) crystals of the JUMBO monochromator⁷ to provide a tunable source of x-ray energies in the range 2700–3400 eV. A VG ADES400 electron spectrometer with low-energy electron diffraction (LEED) capability and a specially constructed high-precision specimen goniometer³ were used for the azimuthal XPD measurements. The Ni crystal and $c(2 \times 2)S$ overlayer were prepared and verified using standard methods described elsewhere.^{1,6} Sulfur $1s$ photoelectrons (binding energy = 2472 eV) were then studied at the three kinetic energies of 230, 500, and 900 eV. The overall energy resolution (including monochromator and analyzer) was approximately 2.0 eV; the angular acceptance was $\pm 2.0^\circ$. Peak

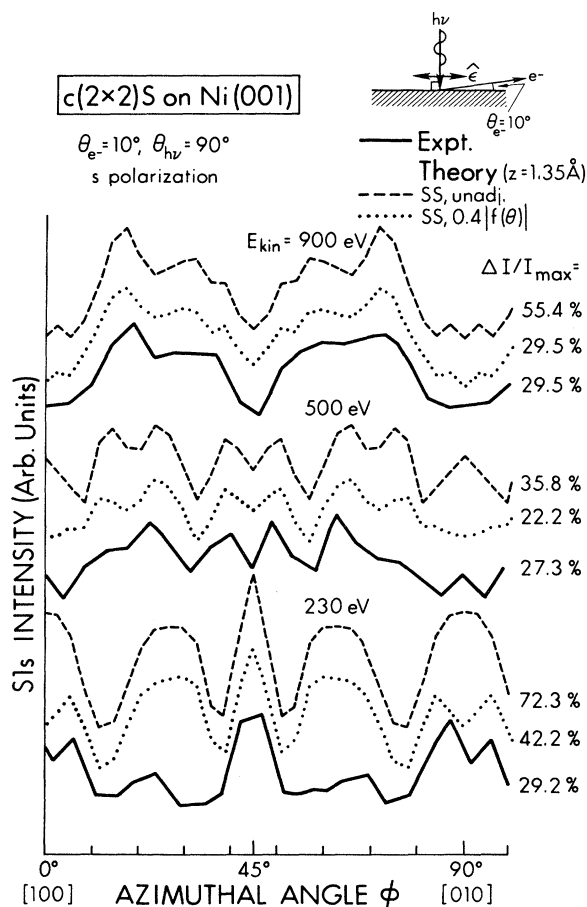


FIG. 1. Comparison of experiment and single-scattering (SS) theory for S 1s azimuthal XPD data in an *s*-polarized geometry and with an electron emission angle of 10° with respect to the surface. Sulfur is assumed to be at 1.35 \AA above the fourfold sites on Ni(001). Electron kinetic energies of 230, 500, and 900 eV are shown. Two types of SS curves are presented: the dashed curves are simple, unadjusted theory with $\beta = \beta' = 1.0$, $\beta'' = 0.0$, and the dotted curves are for empirically optimized choices of $\beta = 0.4$, $\beta' = 0.16$, $\beta'' = 0.0$. Overall anisotropies $\Delta I/I_{\max}$ are given at right.

intensities were determined as areas both by a simple linear background subtraction and a least-squares fit of a Gaussian plus smooth tail; both methods gave the same XPD features, but the latter results are reported here. Two experimental geometries were used, as shown in the insets of Figs. 1 and 2. In both, the photoelectron emission angle is 10° with respect to the surface, and the mean electron collection direction lies in the plane of radiation polarization. In the first geometry, all three energies were explored in *s* polarization (that is, with the polarization vector $\hat{\epsilon}$ lying in the plane of the surface). In the second, a *p*-polarized geometry was chosen in which $\hat{\epsilon}$ was oriented as nearly perpendicular to the electron emission direction as possible, with an angle of 18° between photon incidence and electron exit; only the lowest energy of 230 eV was studied in this geometry. For all cases, full 360° azimuthal scans of the S 1s intensity were made; these were then

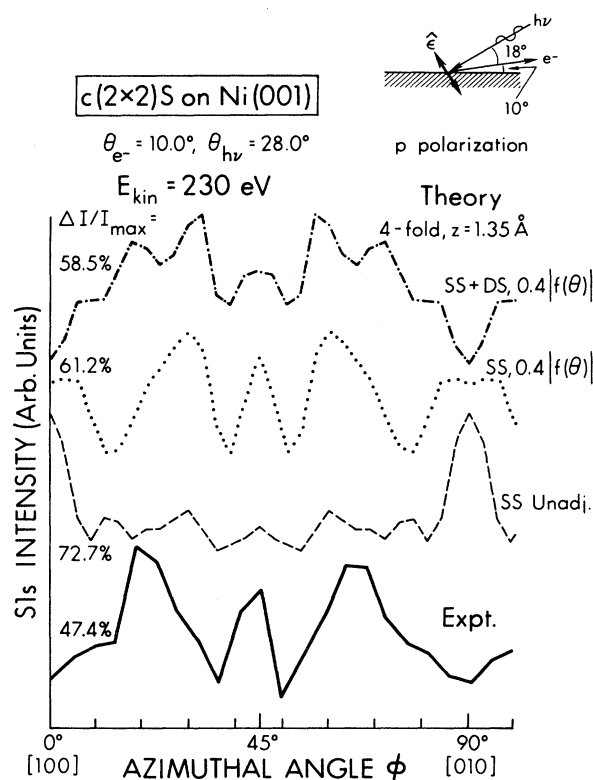


FIG. 2. Comparison of experiment and single-scattering theory for S 1s azimuthal XPD data in a *p*-polarized geometry and with an electron emission angle of 10° with respect to the surface. The electron kinetic energy is 230 eV. Three types of theoretical curves are shown: the dashed curve is unadjusted SS theory with $\beta = \beta' = 1.0$, $\beta'' = 0.0$, the dotted curve is with $\beta = 0.4$, $\beta' = 0.16$, $\beta'' = 0.0$, and the dashed-dotted curve is with the inclusion of double scattering and $\beta = 0.4$, $\beta' = \beta'' = 0.16$.

fourfold-averaged into a single quadrant^{1,3} to reduce noise and check self-consistency against the individual quadrants of raw data. The angles $\phi = 0^\circ, 90^\circ, 180^\circ, \dots$ correspond to emission in $\langle 100 \rangle$ azimuths. Such experimental curves are shown in Figs. 1 and 2. Rather large anisotropies $\Delta I/I_{\max}$ of 27–47% are observed. Figure 2 also makes it clear that changing from *s* to *p* polarization has a very large effect on the XPD pattern observed; the anisotropy also increases by a factor of ~ 1.5 in *p* polarization.

The single-scattering cluster model has been discussed in detail elsewhere,^{1,3} together with its basic assumptions and input parameters for the case at hand. A cluster of ~ 150 atoms was used to ensure full convergence, although ~ 50 atoms normally suffice to produce most of the predicted diffraction features. Scattering factors are obtained from a LEED-type program using a muffin-tin potential.⁸ Inelastic scattering effects are included only in an exponential decay factor for each wave; thus, no polarization or inelastic effects are included in the scattering factors,⁹ although we comment on the possible importance of this latter. In describing the *p*-polarized data, double-scattering events have also been included in some calculations. In allowing for electron refraction at the

surface, the Ni inner potential was set to 10 eV,¹⁰ and that for scattering confined to the *S* was empirically set to 6 eV, a reasonable value in view of the 50% lower planar atomic density of *S* and its relatively large distance above the Ni surface. However, the choice of the *S* inner potential did not strongly affect the predicted curves for all values in the range 4–8 eV. To second order in products of scattering factors, the intensity emitted into a direction \hat{k} is given in this model by^{1,3}

$$I(\hat{k}) \propto |\phi_0|^2 + \beta\phi_0 \sum_j (\phi_j + \phi_j^*) + \beta' \sum_j \sum_{j'} \phi_j \phi_{j'}^* + \beta'' \phi_0 \sum_i \sum_{j(\neq i)} (\phi_{ij} + \phi_{ij}^*), \quad (1)$$

where ϕ_0 is the primary wave in direction \hat{k} (which is taken to be real), ϕ_j and $\phi_{j'}$ are singly scattered waves from atoms j and j' , ϕ_{ij} is a wave doubly scattered from atoms i and j (in that order), and the factors β , β' , and β'' multiplying all interference terms are introduced here as adjustable parameters whose *a priori* choices are $\beta = \beta' = 1.0$, $\beta'' = 0.0$. With few exceptions, the SSC calculations reported previously have used this set of what can be termed unadjusted parameters.^{1–3} The use of $\beta = \beta' = \beta'' = 1.0$ thus represents SSC plus full inclusion all double-scattering events. The sums on i , j , and j' are over all scatterers in the cluster. Each ϕ_j or $\phi_{j'}$ will be proportional to a scattering amplitude $|f_j|$ or $|f_{j'}|$ and each doubly scattered wave will be proportional to some product $|f_i| \cdot |f_j|$. SSC calculations thus normally include the third term of Eq. (1) that is second order in scattering amplitudes, perhaps also corrected with a thermal diffuse scattering term not explicitly shown here.^{1,3} The fourth term is unique to calculations involving double scattering and again is second order in scattering amplitudes. The matrix element describing excitation from a $1s$ subshell into direction \hat{q} will be proportional to $\hat{\epsilon} \cdot \hat{q}$, so that $\phi_0 \propto \hat{\epsilon} \cdot \hat{k}$ and $\phi_j \propto \hat{\epsilon} \cdot \hat{r}_j$ if \hat{r}_j is the direction from emitter to scatterer j .

Before quantitatively comparing experiment and theory, we comment qualitatively on differences expected between the two experimental geometries studied. Because of the $\hat{\epsilon} \cdot \hat{q}$ dependence of the matrix element, the *s*-polarized case should put more emphasis on primary emission toward—and low-angle scattering from—other *S* atoms situated between emitter and detector. Previous XPD studies at higher energies^{1,3} also suggest that, for adsorbates situated ≥ 1.0 Å above the substrate surface, the forward-peaked nature of the scattering factors involved may make it difficult for the substrate to contribute significantly to scattering. Thus, for the present case, the *s*-polarized data might be expected to be less sensitive to adsorbate vertical position z above the fourfold hollow site, at least for values near the 1.3–1.4 Å expected. By contrast, the *p*-polarized geometry selectively directs primary emission toward substrate atoms, while at the same time reducing primary emission in the detection direction, which now lies near a node in $\hat{\epsilon} \cdot \hat{q}$. If $|\phi_a|$ represents the magnitude of a typical wave scattered from an adsorbate atom and $|\phi_s|$ an analogous magnitude for scattering from a substrate atom, this can be stated as

$|\phi_0| \approx |\phi_s| \approx |\phi_a|$. Thus, substrate-scattered waves might be expected to interfere much more strongly with the weakened primary wave, yielding higher z sensitivity. A possible disadvantage of such a geometry, however, is that the relative strengths of all primary and scattered waves must be known more accurately and multiple scattering effects may become more important. In *s* polarization, the situation is reversed; here a strong primary wave interferes with weaker waves scattered from adsorbate and (to a lesser degree) substrate atoms, so that in general $|\phi_0| \gg |\phi_a| > |\phi_s|$. Thus, a kinematical approach is expected to be better in this case.

In Fig. 1, experiment and unadjusted single-scattering theory (that is, with $\beta = \beta' = 1.0$ and $\beta'' = 0.0$) are compared for *s* polarization at the three energies studied. There is generally very good agreement for all energies, with only slight deviations in shape and relative intensity being found at the lowest energy of 230 eV for the symmetry-related features at $\phi \approx 15^\circ$ – 35° and 55° – 75° . These deviations may be due to multiple-scattering effects, which would be expected to be strongest at this lowest energy. Simple theory is found to overestimate the degree of anisotropy in *s* polarization by a factor of ~ 1.8 , but this is typical of such calculations, and several reasons for such discrepancies have been discussed previously^{1,3} (inelastic effects in scattering factors,⁹ curved-wave corrections for near-neighbor scattering,¹¹ and the influence of multiple scattering¹²). This has led to prior suggestions of multiplying each $|f_j|$ in Eq. (1) by a “damping factor,” with numbers of ~ 0.4 – 0.5 appearing to improve agreement with experiment in some prior XPD work.¹ This is most self-consistently done by, for example, choosing $\beta \approx 0.4$ and $\beta' = \beta^2 \approx 0.16$ due to the second-order nature of the third term in Eq. (1); β'' is still left as zero to exclude pure double-scattering terms. Such curves are also shown in Fig. 1, and it is clear that this change both lowers anisotropies to values nearer experiment and improves agreement with experiment as to certain minor features for 500 and 230 eV. However, the overall XPD curves for all three energies are of essentially the same shape for both choices of these parameters. This last observation shows that second-order terms are not strongly significant in producing the XPD patterns in *s* polarization. That is, if all second-order terms are truly negligible, then β' and β'' can be set to zero, and a decrease in β would simply decrease the entire first-order sum in Eq. (1) in such a way that *no* changes in features would be seen. Only the anisotropy would decrease as β is decreased for such a case. That this is very nearly true in Fig. 1 confirms that simple first-order interferences dominate in these *s*-polarization measurements.

Turning now to the question of sensitivity to vertical adsorbate position z , we compare in Fig. 3 experiment and single-scattering curves for different z values from 0.0 Å (in plane) to 1.6 Å (well above plane), with the highest density of curves being around the 1.3–1.4 Å expected.⁶ As anticipated based upon our prior discussion of the *s*-polarized geometry, there is little change in the theory curves over the range 1.3–1.6 Å, although the features at $\phi \approx 15^\circ$ – 35° and 55° – 75° have shapes and positions in slightly better agreement with experiment in going to

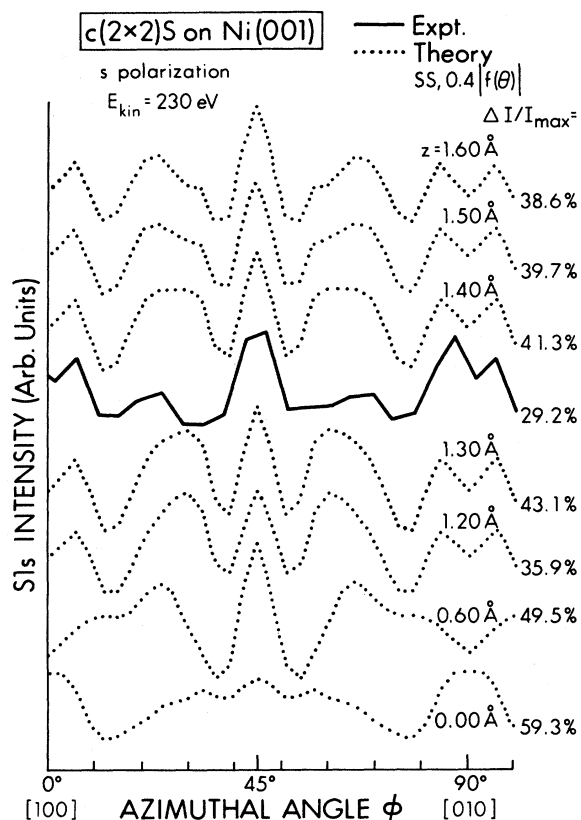


FIG. 3. The *s*-polarized data at 230 eV of Fig. 1 are compared to adjusted SS theory for different *z* positions above the fourfold site. Here, the optimized values of $\beta=0.4$, $\beta'=0.16$, and $\beta''=0.0$ are used, although the corresponding unadjusted SS curves differ very little (cf. discussion of Fig. 1).

1.5–1.6 Å. Nonetheless, this comparison is fully consistent with the structure previously determined for $c(2 \times 2)S$ on $Ni(001)$.⁶ The three curves at lowest *z* of 0.0, 0.6, and 1.2 Å demonstrate the previously mentioned point of much higher sensitivity to *z* for more nearly in-plane adsorption. Thus, in general for systems showing smaller vertical distances, such *s*-polarized azimuthal data combined with simple single-scattering theory should be capable of providing useful structural information.

The *p*-polarized data of Fig. 2 is not amenable to such simple interpretation, however. In this figure, experiment is compared first to unadjusted single-scattering theory [i.e., $\beta=\beta'=1.0$, $\beta''=0.0$ in Eq. (1)], at the expected *z* value of 1.35 Å, and very strong disagreement is seen. In particular, the very intense features at $\phi=0^\circ$ and 90° in theory are minima in experiment. However, the simple expedient of reducing the scattering factor amplitudes in the manner discussed previously (i.e., $\beta < 1.0$, $\beta'=\beta^2$, $\beta''=0.0$) is found to radically change the predicted diffraction patterns, and to markedly improve agreement with experiment. A detailed search of β values shows that maximum agreement is achieved for $\beta \approx 0.3$ – 0.5 (and thus, $\beta' \approx 0.09$ – 0.25). A curve generated for the combination $\beta=0.4$, $\beta'=0.16$ is shown in the figure and it exhibits both a much reduced intensity for the features at

$\phi=0^\circ$, 90° and much more nearly the correct features and relative intensities for the three main experimental peaks between $\sim 15^\circ$ and 75° . The features at $\phi=0^\circ$ and 90° are still predicted to be too strong, however.

Thus, it is clear that second-order effects are much more important in this *p*-polarized geometry, and that the effective scattering factor amplitudes are $\frac{1}{3}$ to $\frac{1}{2}$ of those calculated in the usual way.⁸ These reduction factors thus agree well with prior empirical XPD analyses.¹ Also, reductions of this order are consistent with those calculated theoretically for large-angle scattering in the presence of inelastic effects.⁹ Curved-wave corrections^{2,11} and multiple-scattering effects¹² also may play a role in this effective damping of the $|f_j|$'s, however.

In view of the demonstrated strength of second-order effects in *p* polarization, it is also necessary to consider true double-scattering events as represented in the fourth term of Eq. (1). In this way, all events through second order in $|f_j|$ will be included. This has been done in a manner completely analogous to prior treatments of extended x-ray-absorption fine structure.^{11,12} If each scattering factor amplitude is again scaled by a variable factor, then the most self-consistent choice of β values is $\beta \leq 1.0$, $\beta'=\beta''=\beta^2$. A large series of such calculations were performed for various *z* positions, with β being varied from 1.0 down to 0.2. The best agreement with experiment is found for $\beta=0.3$ – 0.4 (and thus $\beta'=\beta''=0.09$ – 0.16), and such a theoretical curve is shown in Fig. 2. Including double scattering significantly improves agreement near $\phi=0^\circ$ and 90° , where minima now correctly appear. The overall shape of the two main peaks at $\phi=30^\circ$ and 60° is also closer to experiment, although their positions still differ by $\sim 10^\circ$ from experiment. The only negative effect of including double scattering is that the peak at $\phi=45^\circ$ is weakened too much in relative intensity. Thus, it is clear that a reduction in effective scattering amplitudes is observed in *p* polarization and that higher-order scattering effects must be accurately included in order to correctly predict the observed diffraction features. This is not surprising in view of our earlier comments concerning the relative wave strengths involved for this geometry.

Even though it thus may be necessary to use a full multiple-scattering approach^{4,5} to quantitatively describe such *p*-polarized data, it is useful to ask what approximate *z* sensitivity is expected based upon the empirically adjusted double-scattering calculations. Figure 4 thus compares experiment with theory for the same *z* values as Fig. 3. The theory curves are here found to be very sensitive to *z*, especially for the region from 1.20 to 1.50 Å that is rather insensitive for the *s*-polarized case (cf. Fig. 3). The best overall agreement between theory and experiment is for $z=1.45$ – 1.50 Å, inasmuch as the positions of the two most prominent features in experiment at $\phi=21^\circ$ and 66° are better predicted, with theory showing them to be at $\phi=19^\circ$ and 71° ; also, the peak at $\phi=45^\circ$ has approximately the correct relative intensity, although it is a little too intense relative to experiment. The agreement for $z=1.30$ – 1.35 Å is not as good, although the principal diffraction features are at least qualitatively predicted (cf. also Fig. 2). There is also a rather abrupt change in

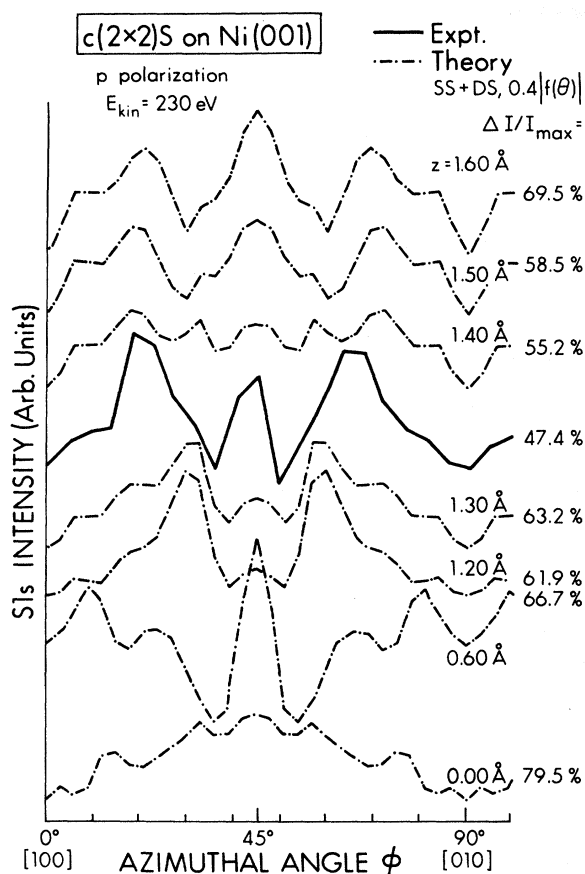


FIG. 4. The p -polarized data at 230 eV of Fig. 2 are compared to theoretical curves including both single and double scattering and with optimized scattering factor amplitudes. Here, $\beta = 0.4$, $\beta' = 0.16$, and $\beta'' = 0.16$.

predicted features between 1.30 and 1.50 Å, a range which overlaps the expected true z value for S on Ni(001). It is thus not possible to determine the S z position with high precision from this comparison, but the range 1.40 ± 0.10 Å certainly spans the region of best agreement. This

range also is consistent with prior structural determinations for this system.⁶

In conclusion, the 200–900-eV energy range seems very promising for such grazing-emission azimuthal photoelectron diffraction studies. Large anisotropies of ~ 30 – 50 % are observed, and these are found to be very sensitive to polarization for the two extreme cases studied here. In s polarization, a simple single-scattering analysis is found to describe the data rather well, and second-order effects are not very important. Although the z sensitivity in this case is not high, the use of other polarization geometries to better emphasize substrate scattering and/or application to more nearly in-plane or below-plane adsorption systems should enhance this sensitivity. By contrast, in the particular p -polarization geometry studied the primary wave is reduced in relative strength, and second-order scattering effects are clearly important. It is observed that the effective scattering amplitudes are reduced by a factor of $\frac{1}{3}$ to $\frac{1}{2}$ relative to scattering amplitudes calculated in a simple muffin-tin potential, with a major cause of this probably being inelastic effects during scattering. Calculations including double-scattering events as well are found to agree better with the p -polarized data. These calculations are consistent with $z = 1.4 \pm 0.1$ Å for fourfold $c(2 \times 2)$ S or Ni(001), thus also agreeing with prior structural determinations. However, definitive analysis of the p -polarized data may require a full multiple-scattering treatment.

We are indebted to the staff of the Stanford Synchrotron Radiation Laboratory and especially to S. M. Goldberg, J. Yang, and B. Pate for technical assistance during our experimental work. We also thank B. K. Teo for providing us with tables of polarization-corrected scattering factors. The Stanford Synchrotron Radiation Laboratory is supported by the National Science Foundation through the Division of Materials Research. This work was supported by the National Science Foundation (under Grant No. CHE-80-21355), the Commissariat à l'Énergie Atomique (France), and North Atlantic Treaty Organization (Grant No. 260.80).

*Present address: Institut für Physik, Technische Universität München, D-8046 Garching bei München, West Germany.

¹S. Kono, S. M. Goldberg, N. F. T. Hall, and C. S. Fadley, Phys. Rev. B **22**, 6085 (1980); P. J. Orders, R. E. Connelly, N. F. T. Hall, and C. S. Fadley, *ibid.* **24**, 6163 (1981), and references therein.

²L.-G. Petersson, S. Kono, N. F. T. Hall, C. S. Fadley, and J. B. Pendry, Phys. Rev. Lett. **42**, 1545 (1979).

³C. S. Fadley, in *Progress in Surface Science*, edited by S. G. Davison (Pergamon, New York, 1984).

⁴H. H. Farrell, M. M. Traum, N. V. Smith, W. A. Royer, D. P. Woodruff, and P. D. Johnson, Surf. Sci. **102**, 527 (1981), and references therein.

⁵W. M. Kang *et al.*, Phys. Rev. Lett. **47**, 931 (1981).

⁶J. E. Demuth, D. W. Jepsen, and P. M. Marcus, Phys. Rev.

Letts. **32**, 1182 (1974); D. H. Rosenblatt *et al.*, Phys. Rev. B **23**, 3828 (1981); S. Brennan, J. Stöhr, and R. Jaeger, *ibid.* **24**, 4871 (1981).

⁷Z. Hussain, E. Umbach, D. A. Shirley, J. Stöhr, and J. Feldhaus, Nucl. Instrum. Methods **195**, 115 (1982).

⁸J. B. Pendry, *Low Energy Electron Diffraction* (Academic, London, 1974). The program MUFPO by J. B. Pendry was used for calculating scattering factors.

⁹G. Beni, P. A. Lee, and P. M. Platzmann, Phys. Rev. B **13**, 5170 (1976); B. K. Teo and P. A. Lee, J. Am. Chem. Soc. **101**, 2815 (1979); B. K. Teo (private communication).

¹⁰J. E. Demuth, P. M. Marcus, and D. W. Jepsen, Phys. Rev. B **11**, 1460 (1975).

¹¹P. A. Lee and J. B. Pendry, Phys. Rev. B **11**, 2795 (1975).

¹²B. K. Teo, J. Am. Chem. Soc. **103**, 3990 (1981).